Quantitative comparison of hydraulically induced fractures under continuous and cyclic injection on Pocheon granite

Comparaison quantitative des fractures induites par voie hydraulique sous injection continue et cyclique dans le granite de Pocheon.

Melvin B. Diaz, SungGyu Jung
Geotechnical & Geo-space engineering, University of Science and Technology, Republic of Korea, mdiaz@kict.re.kr

Li Zhuang, Kwang Yeom Kim, Hyu-Soung Shin,
Geotechnical engineering division, Korea Institute of Civil Engineering and Building Technology, Republic of Korea

Ki-Bok Min
Faculty member, Department of Energy Resources Engineering, Seoul National University, Republic of Korea

ABSTRACT: A sequence of hydraulic fracturing laboratory experiments using Pocheon granite was carried out to assess and characterize fracture development under monotonic and cyclic water injection. The cylindrical rock specimens were cored with a geometry of 50 mm and 100 mm in diameter and height respectively, with a centered bore hole drilled along its vertical axis. A CT scan was used for fracture inspection and data acquisition after rock failure. Arithmetic average height, maximum height of the profile, length of the curve, and tortuosity were taken as fracture parameters for later comparison. The results indicate that the total length of the fractures decreases with increasing number of cycles, while the tortuosity increases.

RÉSUMÉ : Une série d'expériences de laboratoire de fracturation hydraulique en utilisant le granite de Pocheon a été réalisée pour évaluer et caractériser le développement de la fracture sous l'injection d'eau monotone et cyclique. Les éprouvettes de roche cylindrique ont été carottées d'une géométrie de 50 mm et 100 mm de diamétre et de hauteur respectivement, avec un alésage centré percé tout au long de son axe vertical. Une tomographie assistée par ordinateur (CT) a été utilisée pour l'inspection des fractures et l'acquisition des données aprés la défaillance d'une roche. La hauteur moyenne arithmétique, la hauteur maximale du profil, la longueur de la courbe et la tortuosité ont été prises comme paramétres de rupture pour une comparaison ultérieure. Les résultats indiquent que la longueur totale des fractures diminue avec le nombre croissant de cycles, tandis que la tortuosité augmente.

KEYWORDS: Cyclic injection, hydraulic fracturing, fracture development, tortuosity, length of the fracture.

1 INTRODUCTION

Induced seismicity associated to fluid injection at high pressures for reservour stimulation has raised communities and project managers concern about the feasabilty of such kind of activities. A wellknown case is the geothermal project in the city of Basel, Switzerland where the levels of triggered events led to the end of the project that aimed at heat mining for electricity generation (Deichmann and Giardini 2009). Although no seismic events associated with fluid injection at great depths has reported significant damage to properties, there is a clear need for better project managemnt that should includ a induced seismicity protocol as well as a strong community information programme (Majer et al. 2007). At the same time, the development of technologies that could achieve permeability enhacement of the reservor while reducing the seismic events is desirable.

In this respect, the concept of cyclic stimulation was presented by Zimmermann et al. (2009), where a stimulation program was implemented in a geothermal project in Germany and proved to increase productivity. Later, a numerical study where a similar idea of fatigue hydraulic fracturing by cyclic stimulation was presented as a safe alternative to reduce the number of significant seismic events during reservoir permeability enhancement (Zang et al. 2013). The authors created a numerical model that included natural fractures evaluated in two scenarios, and found a decrement on the seismic energy release.

Motivated by the aforementioned reports, laboratory experiments have also evaluated the applicability of this concept. In fact, Patel et al. (2016) reported an increment on fracture permeability in Tennessee sandstone after cyclic injection along with a decrement in breakdown pressure. Also, they reported an influence zone near the main fracture with the occurrence of thinner fractures.

Similarly, Zhuang et al.(2016) carried out experiments on granite rock specimens, and reported a threshold limit at around 76% to 82% of the breakdown pressure under monotonic loading. Fracture development was said to present branches especially when the number of cycles was higher. However no fracture size assessment was carried out to compare influence of the number of cycles.

In this study, a series of hydraulic fracturing laboratory experiments using cylindrical granitic specimens was carried out to assess fracture development by comparing four fracture parameters. The fractures were inspected with a CT scan, and the calculations were based on voxel data images.

2 TESTING MATERIAL AND EXPERIMENTAL SETUP

2.1 *Granitic rock.*

The rock material employed in this sequence of laboratory hydraulic fracturing tests was a Jurasic granite obtained from Pocheon, South korea. Volumetric mineral composition, porosity, as well as longitudinal wave velocity, and indirect tensile strength of this granite are listed in Diaz et al. (2016a). It is worth mentioning that since granitic rocks are characterized by three nearly orthogonal planes of weakness, the measurements aforementioned reported different values along each plane. That is the case of the Brazilian Tensile Strength (BTS) test that reported values of 6.1, 8.2, and 8.8 MPa for the rift, grain, and hardway planes, respectively.

2.2 *Hydraulic fracturing samples and testing conditions.*

Seven cylindrical rock samples of 10 cm in heigth, and 5 cm in diameter were prepared for this sequence of hydraulic fractuirng tests. All samples include a midpoint circular hole with a diameter of 8 mm that crosses them from top to bottom along their longest axis. The samples were cored perpendicular to the hardway plane of Pocheon granite, leaving both rift and grane planes mutually perpendicular and along the vertical axis of each specimen.

The testing equipment, plus the X-ray computed tomography (CT) scanner used in this study are the same occupied and described by Diaz et al. (2016a), with the granitic sample sitting on a pedestal with its longest axis along the vertical direction. Confining and vertical pressures were applied independently.

The experimental testing conditions established for this sequence of hydro-fracturing tests are as follows: vertical pressure of 10 MPa applied through a servo-hydraulically controlled piston, confining pressure of 5 MPa provided by additional oil line supply, and water as the injected fluid.

A summary of the type of loading, number of cyclic loadings before breakdown, pressurization rate and breakdown pressure for the seven samples is given in Table 1. The samples are organized according to the number of loading cycles borne before failure. The first two rock specimens were failed under monotonic loading conditions, while the rest were loaded under cyclic conditions with 10.2 MPa as the upper limit, established as the 90% of the average of the first two. Note that samples 6 and 7 did not failed under cyclic conditions, thus they were failed under monotonic loading.

Table 1. Sample number, breakdown pressure and other hydro-fracturing testing conditions.

Sample	*Loading*	*No. cycles*	*pressurization rate(MPa/s)*	*Breakdown pressure(MPa)*
1	monotonic	-	0.1	11.25
2	monotonic	-	0.1	11.46
3	cyclic	2	0.1	10.2
4	cyclic	43	0.1	10.2
5	cyclic	65	0.1	10.2
*6**	cyclic	107*	0.1	10.2*
*7**	cyclic	150*	0.1	9.58*

* Cyclic loading stopped due to absence of failure, therefore loaded monotonically.

3 FRACTURE DATA ACQUISITION

After failure, i.e., the generation of hydraulic fracture, the samples were taken for CT scan inspection. In general water injection created nearly bi-wing fractures. To compare different characteristics of the fractures, we extracted cross sections or slice images at the midpoint of the height of the created fracture within each sample. Figure. 1 presents X-ray images with inverted CT values to help distinguish the fractures. The nomenclature “a” and “b” refers to the relative location of the fracture in either the superior or inferior half.

The general orientation of the fractures results from their propagation along the least strong plane of weakness (rift), and it is also influenced by local heterogeneity within the sample (Diaz et al. 2016a). As an example, fracture 2a departs around 30˚ degrees from the rift plane. Similarly, fracture 6a is deviated around 5˚ degrees, and its counterpart fracture 6b started along the weakest plane but later deviated due to local heterogeneity of the rock matrix. The rest of fractures developed practically parallel to the rift plane of weakness.

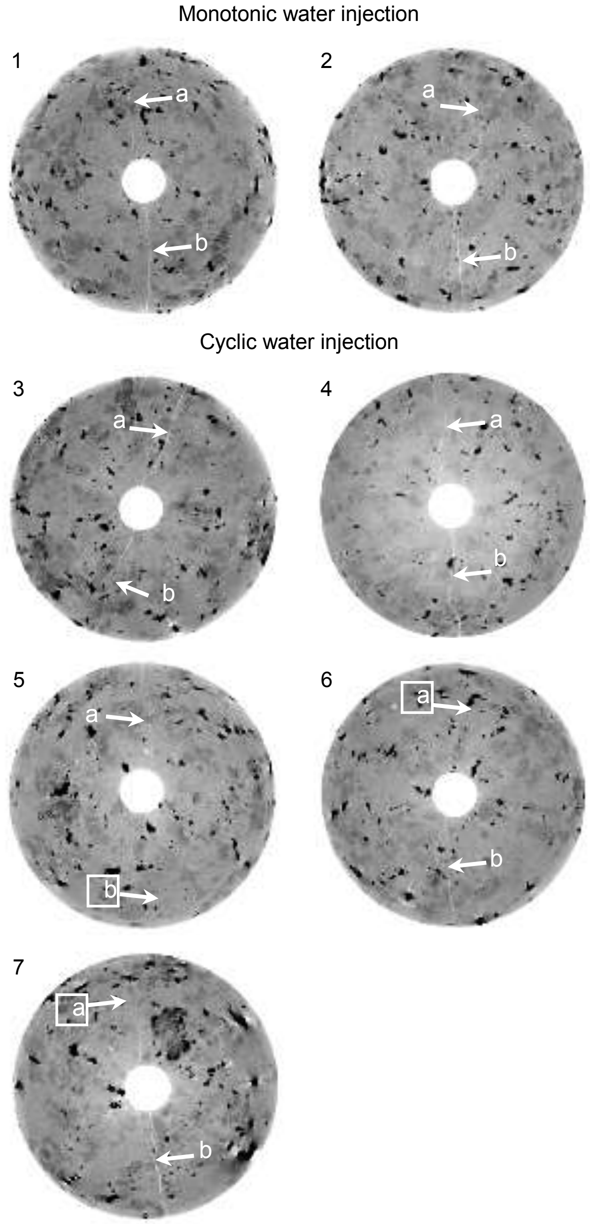

Figure 1. Cross sectional X-ray images of 7 cylindrical granite samples with inverted intensity values. The cross sections were taken at half the height of the created fracture, and letters “a” and “b” show complete fractures in the upper and lower half respectively. Legend in a box indicates the end of a non-completely extended fracture.

Fractures 5b, 6a, and 7a did not reached the outer surfaces of the specimen, and they are indicated in Figure 1 with their designation written in a square frame. This three cases occurred only during cyclic injection, although the same pressurization rate was applied to all cases. It seems that fracture development occurred unevenly, and it is attributed to local heterogeneity.

Furthermore, CT images also served to generate 2D coordinates of multiple points along the fracture boundary, spaced approximately every 0.25 mm (Figure 2). A total of 14 sets of fracture coordinates were obtained, two per sample, and they were used for subsequent calculations of four fracture parameters as a way to compare fracture advancement. Although 3D fracture acquisition is desirable, this was limited by the fracture thinness. The computation of the 2D fracture parameters, which are described later, was implemented through a computer algorithm developed for this purpose.

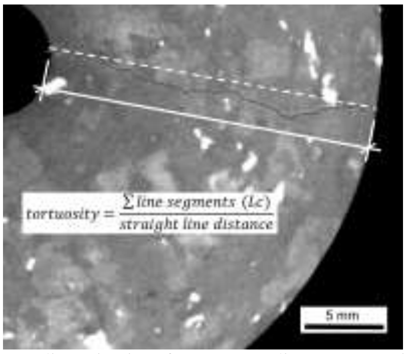

Figure 2. Fracture discretization for 2D coordinates extraction along sample cross section, and tortuosity description. Modified after Diaz et al. (2016a), Fig. 4.

The selected parameters for fracture comparison are: arithmetic average height (R_a), maximum height of the profile (R_t), length of the curve (L_c), and tortuosity (t). The first two parameters measure the average height of the fracture profile with respect to the central line, and the vertical distance from the highest and lowest points of the profile respectively (Gadelmawla et al. 2002). The last two are illustrated and explained in Figure 2, where the length of the curve was computed as the sum of liner segments along the fracture margin, while tortuosity is taken as the ratio between the length of the curve and the straight line distance between fracture start and end. In addition R_a, R_t, and L_c have units in mm, while tortuosity is non-dimensional.

4 RESULTS AND DISCUSSION

The measured results of four fracture parameters are listed in Table 2. Arithmetic average height (Ra), maximum height of the profile (Rt), length of the curve (Lc), and tortuosity (t) are given for upper (a) and lower (b) fractures. Furthermore, as mentioned previously, fractures 5b, 6a, and 7a ended before reaching the external surface of the cylindrical rock specimens.

For the case of monotonic water injection, fracture in samples 1 and 2 reached surface, and their length of curves are higher than 21 mm. However only fractures in sample 1 yield similar values, while Ra and Rt are different for fractures in sample 2. In fact, fracture 2a has a higher average height, and maximum height along its profile, and as mentioned earlier it diverged around 30˚ degrees from the rift plane.

During cyclic water injection, only fractures within specimens 3 and 4 developed completely and reached the rock cored surface. These samples failed at 2 and 43 cycles respectively. In contrast, the remaining three specimens only fully developed one fracture, for which the length of curve was also higher than 21 mm.

The arithmetic average height (Ra) for all fractures appears to follow no trend, leaving the values into a range from 0.15 mm to 0.47 mm corresponding to fractures 2b and 4b respectively.

In similar fashion, the maximum height of the profile (Rt) shows no defined tendency and yields a range of measures from 0.81 mm to 1.87 mm, corresponding again to fractures 2b and 4b respectively. The rest of measured maximum heights fall into this range.

For the length of the curve, we decided to add both values from upper and lower fractures within each sample, as a way to compare the total length of fracture, and plot them against the number of cycles before failure. This arrangement is shown in Figure 3.

Table 1. Computed values of four 2D fracture parameters: arithmetic average height (R_a), maximum height of the profile (R_t), length of the curve (L_c), and tortuosity (t).

Fracture	R_a (mm)	R_t *(mm)*	L_c *(mm)*	*t* *(--)*
1a	0.26	1.38	22.79	1.048
1b	0.26	1.16	22.77	1.051
2a	0.43	1.73	21.99	1.055
2b	0.15	0.81	21.53	1.053
3a	0.27	1.33	23.26	1.052
3b	0.27	1.40	22.66	1.043
4a	0.45	1.79	21.83	1.055
4b	0.47	1.87	21.89	1.057
5a	0.22	1.54	22.47	1.075
*5b**	0.26	1.49	19.30	1.045
*6a**	0.32	1.57	13.87	1.085
6b	0.34	1.43	22.42	1.051
*7a**	0.23	0.95	13.28	1.040
7b	0.18	0.92	21.35	1.053

* Fractures that did not reach the outer surface.

Moreover, we have also added tortuosity on a second axis to contrast their development as the number of cycles increased. This time tortuosity was taken only from one of the fractures per sample, those that developed completely from the borehole to the outer granite cylindrical specimen.

Interestingly, the total length of the fracture plotted with its vertical axis on the left, shows a decreasing trend with increasing number of values, which results in a ratio of -0.0733 mm/cycle. This result suggest that although cyclic injection lowers the pressure required for rock failure, it also influences the total extend of the fracture, with less developed fractures at higher number of cycles.

At the same time, tortuosity exhibits a different behavior, with an increasing pattern for the first half and lower values in the second. At this point, it is important to recall that the last two samples (6 and 7) did not fail during cyclic water injection, and therefore were failed under monotonic injection.

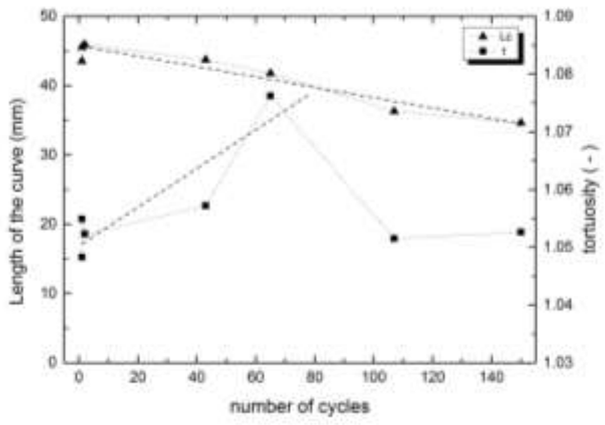

Figure 3. Length of curve and tortuosity plotted against number of loading cycles before failure. Here, the value of the length of curve corresponds to the sum of both fractures per sample. On the other hand, tortuosity represent only one fracture per sample because in some cases the fracture did not reach the outer surface.

This is the reason why the last two tortuosity measures were not included for trend line calculation. This second trend line suggest that as the number of water injection cycles increases, the fluid has more time to penetrate the rock matrix and create new courses by connecting preexisting microfractures that result in higher tortuosity values. In fact, a study conducted to measure the tensile strength of this granite found that the surface roughness of the tensile plane of failure is greatly influenced by the preexisting microcracks, as well as grain size and mineral strength in a small scale (Diaz et al. 2016b). Moreover, Zhuang et al. (2016) also pointed out that cyclic injection produces more branched fractures especially at higher number of cycles.

To understand the evolution of hydraulic fracturing under cyclic injection, more work needs to be done. Further analysis of complete 3D fractures is desirable, and they will be considered in forthcoming publications.

5 CONCLUSIONS

A sequence of hydraulic fracturing laboratory experiments on Pocheon granite was carried out to measure fracture evolution under monotonic and cyclic water injection. All samples have a cylindrical shape with a height of 10 cm, and a diameter of 5 cm. A hole drilled from top to bottom mimics the borehole with a diameter of 8 mm. All tests were conducted under a vertical pressure of 10 MPa, a confining pressure of 5 MPa, and a pressurization rate of 0.1 MPa/s.

After failure, the cylindrical rock samples were scanned with the aid of an X-ray CT equipment, in order to extract fracture features for later computations. It was observed that most specimens developed bi-wing fractures parallel to the rift plane of weakness of the granite.

To compare fracture evolution within each specimen, arithmetic average height, maximum height of the profile, length of the curve, and tortuosity were chosen as fracture parameters. The results indicate that average and maximum height along the fracture profiles have no clear tendency, rather they give a clear range of values per parameter.

On the other hand, the total length of the fracture that included both wings, decreases as the number of cyclic loadings increases with a ratio of -0.0733 mm/cycle. In addition, the tortuosity showed a two stage development with an increasing trend in the first part as the number of cycles increased.

6 ACKNOWLEDGEMENTS

This research was supported by a grant (No. 20133030000240) from the New and Renewable Energy Program of the Korea Institute of Energy Technology Evaluation and Planning, funded by the Ministry of Trade, Industry and Energy of the Korean Government and a grant (No. N0002098) from the International R&D Program funded by Korea Institute for Advancement of Technology.

7 REFERENCES

Deichmann N. and Giardini D. 2009. Earthquakes induced by the stimulation of an enhanced geothermal system below Basel (Switzerland). *Seismological Research Letters*, 80(5), 784-798.

Diaz M.B., Jung S.G., Zhuang L., Kim K.Y., Yeom S. and Shin H.S. 2016. Effect of cleavage anisotropy on hydraulic fracturing behavior of Pocheon granite. In *50th US Rock Mechanics/Geomechanics Symposium*. Houston, Texas, USA (26-29 June), no. 16-143, American Rock Mechanics Association.

Diaz M.B., Jung S.G., Zhuang L., Kim K.Y., Jung J.H. and Shin H.S. 2016. Tensile strength anisotropy of Pocheon granite and roughness evaluation of its failure planes. *Rock Mechanics and Rock Engineering: From the Past to the Future* (1), 135.

Gadelmawla E.S., Koura M.M., Maksoud T.M.A., Elewa I.M. and Soliman H.H. 2012. Roughness parameters. *Journal of Materials Processing Technology*, 123(1), pp.133-145.

Majer E.L., Baria R., Stark M., Oates S., Bommer J., Smith B. and Asanuma H. 2007. Induced seismicity associated with enhanced geothermal systems. *Geothermics* 36(3), 185-222.

Patel S., Sondergeld C. and Rai C. 2016. Laboratory studies of cyclic injection hydraulic fracturing. In *SEG Technical Program Expanded Abstracts 2016, Society of Exploration Geophysicists* 3364-3368.

Zang A., Yoon J.S., Stephansson O. and Heidbach O. 2013. Fatigue hydraulic fracturing by cyclic reservoir treatment enhances permeability and reduces induced seismicity. *Geophysical Journal Internationale* ggt301.

Zimmermann G., Moeck I. and Blöcher G. 2010. Cyclic waterfrac stimulation to develop an enhanced geothermal system (EGS)—conceptual design and experimental. *Geothermics* 39(1), 59-69.

Zhuang L., Kim K.Y., Jung S.G., Diaz M.B., Min K.B., Park S., Zang A., Stephansson O., Zimmerman G. and Yoon J.S. 2016. Laboratory study on cyclic hydraulic fracturing of Pocheon granite in Korea. In *50th US Rock Mechanics/Geomechanics Symposium*. Houston, Texas, USA (26-29 June), no. 16-163, American Rock Mechanics Association.